Formation of a yeast SNARE complex is accompanied by significant structural changes

Luke M. Rice[a], Patrick Brennwald[b], Axel T. Brünger[a,*]

[a]*The Howard Hughes Medical Institute, and Department of Molecular Biophysics and Biochemistry Yale University, New Haven, CT 06520, USA*
[b]*Department of Cell Biology and Anatomy Cornell University Medical College 1300 York Avenue, New York, NY 10021, USA*

Received 14 August 1997; revised version received 20 August 1997

Abstract The evolutionarily conserved SNARE (SNAP receptor) proteins and their complexes are key players in the docking and fusion of secretory vesicles with their target membrane. Biophysical techniques were used to characterize structural and energetic properties of the cytoplasmic domains of the yeast SNAREs Snc1 and Sso1, of the SNAP-25-like domain of Sec9, and of the Sso1:Sec9 and Sso1:Sec9:Snc1 complexes. Individually, all three SNAREs are monomeric; Sso1 shows significant secondary structure while Snc1 and Sec9 are largely unstructured. Ternary SNARE complex formation ($K_D < 50$ nM) is accompanied by a more than two-fold increase in secondary structure. This binding induced structure, the large increase in thermal stability, and the self-association of the ternary complex represent conserved properties of SNAREs that are probably important in vesicle docking and fusion.

Key words: Circular dichroism; Fusion; Exocytosis; Yeast; Structural change

1. Introduction

Intracellular membrane fusion is mediated by a complex and as yet poorly understood sequence of protein-protein interactions orchestrated by a set of conserved proteins. In neuronal exocytosis, these include the plasma membrane associated proteins syntaxin and SNAP-25, and the vesicular protein synaptobrevin (also referred to as VAMP). Each of these proteins represents a small protein family with distantly related members apparently expressed in all eukaryotic cells (for review, see [1,2]).

While the function of these protein families in membrane fusion is not understood, the biochemical properties of the neuronal proteins have been studied in some detail. It was shown that these three proteins spontaneously assemble into a stable ternary complex [3–6] which can recruit a member of the SNAP (soluble NSF attachment protein) family. Recruitment of SNAPs allows recruitment of NSF (*N*-ethylmaleimide sensitive fusion protein, Sec18 in yeast), an ATPase that catalyzes the temporary dissociation of the ternary SNARE complex [3,5,7,8].

The SNARE hypothesis postulates that the SNARE proteins are responsible for the specificity in vesicular transport [3,9], and that the mechanism by which specific fusion is achieved is conserved throughout the eukaryotic kingdom. According to this model, each transport vesicle carries a particular SNARE (v-SNARE), and each acceptor membrane carries another SNARE (t-SNARE). Specific interactions between v- and t-SNARE(s) would be the mechanism by which docking selectivity is achieved. Certain aspects of the SNARE hypothesis have recently become the subject of some debate, largely because of results obtained from the in vitro reconstitution of homotypic vacuole fusion [10,11] and because of the isolation of SNARE complexes on purified vesicles [12].

The sequence conservation between evolutionarily removed members of the syntaxin, SNAP-25, and synaptobrevin gene families is quite limited. If SNARE proteins indeed operate by a similar mechanism, then the structural properties of distantly related SNARE proteins and their complexes should be more similar than the primary sequence would suggest. Structural and conformational changes during SNARE assembly and disassembly may form the basis of membrane fusion, and therefore should be highly conserved. It is therefore essential to discover whether sets of distantly related SNARE proteins are structurally similar and/or undergo similar assembly-disassembly reactions. Comparative studies of this kind may prove instrumental in establishing a common and basic mechanism by which these proteins operate.

In order to identify potentially conserved structural and energetic hallmarks of SNARE proteins, an extensive biophysical characterization of the yeast SNARE proteins Sso1 [13], Sec9 [14], and Snc1 [15,16], was performed. Two of the three SNAREs are largely unstructured in vitro, and major structural changes occur when SNAREs bind each other to form stable complexes. Estimated dissociation constants for the Sso1:Sec9 and the Sso1:Sec9:Snc1 complexes were unexpectedly high. Examination of the oligomerization state of individual proteins and their complexes revealed multimerization of the ternary complex. Tight binding, binding induced structure, and multimerization of the ternary complex are properties that are likely to play an important role in the docking/fusion process.

2. Materials and methods

2.1. SNAP-25-like domain of Sec9 gene synthesis

Eight overlapping single-stranded oligonucleotides were synthesized to cover the entire coding region of the SNAP-25-like domain of Sec9 (residues 401–651). Codons used less than 14% (for a particular amino acid) of the time in genes from Gram-negative bacteria were replaced with more favorable ones. A total of 77 codons were replaced. The sequences of the eight oligonucleotides were as follows:

*Corresponding author. Fax: +1 (203) 432-6946.
E-mail: axel.brunger@yale.edu

Abbreviations: CD, circular dichroism; NSF, *N*-ethylmelamide sensitive factor; SNAP, soluble NSF attachment protein; SNARE, SNAP receptor; NMR, nuclear magnetic resonance; DTT, dithiothreitol; SNAP-25, synaptosomal associated protein of 25 kDa; VAMP, vesicle associated membrane protein; IPTG, isopropylthiogalactoside; GST, glutathione-*S*-transferase; SDS, sodium dodecyl sulphate; EDTA, ethylenedinitrilo tetraacetic acid; PMSF, phenylmethylsulphonylfluoride; PCR, polymerase chain reaction

PII S0014-5793(97)01091-0

(1) cccgggatccatatggctcagcgtggttacaaaacctttgaagaaatccagaaagaagaggaggctcgccagcagcaggaagaagatgaagcagtagatgaaatc.
(2) ccagggtgttcatacctgcacgttccgcgtcctgagccattttcagggtgttgcgagtagaagctacggaagactgtttagtaaatttgatctcctgcttgatttcatctactgcttcat.
(3) tgcaggtatgaacaccctgggtatgctgggtcatcaatctgaacagctgaacaacgtagaaggtaacctggatctgatgaaggtgcaaaacaaagttgcagatgaaaaagttgcagaact.
(4) tttacggttcttcagctgctcttcacgctcgcgacgacggcgcttggagttaaacgggttagaaacatgtacagccaggatagaacggttcagttttttcagttctgcaactttttcatc.
(5) agcagctgaagaaccgtaaaattgaagaaaaactgatgcgcgagcaaaccagccagcaactgtctcagtccactcaacgtatcgagggtgctatgaacgcaaacaacaacatcagcgagg.
(6) cgatcaatttccagttccatttcgtcatcttcttcatcgttctcaaactgataacgctttgccttttccagaacgttcttacgctgatagcgttcacgcacctcgctgatgttgttgttt.
(7) atggaactggaaattgatcgcaacctggaccagattcagcaggttagcaaccgtctgaagaaaatggctctgaccactggtaaagaactggactctcagcaaaaacgtctcaacaacatt.
(8) cccggatccctcgagttaacggatacctgccagacggttggtgttcatgtgcaggttgatatccagatcatcagtgctttcctcaatgttgttgagacgtttttg.

In the first reaction, oligonucleotides (1) and (2), (3) and (4), (5) and (6), and (7) and (8) were pairwise combined and extended using either Klenow fragment (New England Biolabs) or Pfu polymerase (Stratagene). Then, the overlapping, double-stranded products of the first two reactions ((1)+(2) and (3)+(4)) were combined and PCR amplified with Pfu polymerase using oligonucleotides (1) and (4) as primers. A similar reaction was performed for the overlapping, double-stranded products of the second two reactions using oligonucleotides (5) and (8) as primers. Finally, the overlapping, double-stranded products of these two reactions were combined and PCR amplified using oligonucleotides (1) and (8) as primers. The DNA sequence was verified by dideoxy sequencing performed by the W.M. Keck Foundation Biotechnology Resource Laboratory at Yale University.

2.2. Recombinant expression and purification

The cytoplasmic domains of Sso1 (residues 1–265) and Snc1 (residues 1–93) were cloned into the GST fusion vector pGEX4T-1 (Pharmacia), and the SNAP-25-like domain of Sec9 was cloned into pGEX5X-3 (Pharmacia). Proteins were expressed in BL21 cells grown in Terrific broth. Cells were pelleted by centrifugation, re-suspended in lysis buffer (20 mM Tris pH 8.0, 250 mM NaCl, 5 mM EDTA, 2.5 mM DTT, and 1 mM PMSF), and lysed by sonication. After clarification of the lysate by centrifugation, the supernatant was mixed with approximately 8 ml of glutathione sepharose 4B (Pharmacia) for 30 to 60 min. The beads were batch washed with lysis buffer, and with either thrombin buffer (20 mM Tris pH 8.0, 50 mM NaCl) for Sso1 and Snc1, or with Factor Xa buffer (20 mM Tris pH 8.0, 150 mM NaCl, 1 mM $CaCl_2$) for the SNAP-25-like domain of Sec9. 20 ml of the appropriate protease buffer was added to the beads, then either thrombin (Haematologic Technologies) or Factor Xa (Haematologic Technologies) for overnight cleavage with mixing at 4°C. The beads were then collected and washed twice, and the supernatant applied directly to an ion exchange column. Sso1 and Snc1 were purified on a Mono-S (Pharmacia) cation exchange column. The SNAP-25-like domain of Sec9 was purified on a Mono-Q (Pharmacia) anion exchange column and then on a Superdex 75 (Pharmacia) size exclusion column. The purifications resulted in very pure proteins as assessed by Coomassie (Fig. 1) and silver stained SDS gels (not shown). For purification of the binary and ternary complexes, equimolar amounts of the appropriate proteins were mixed and incubated for 1 to 2 h, and then applied to a Mono-Q anion exchange column.

2.3. Size exclusion chromatography and multi-angle laser light scattering

Analytical size exclusion chromatography coupled with multi-angle light scattering was performed at 4°C using a Superdex 200 10/30 gel filtration column (Pharmacia) equilibrated in 20 mM Tris pH 8.5, 300 mM NaCl and a Mini-DAWN light scattering detector (Wyatt Technologies) with an attached interferometric refractometer (Wyatt Technologies) for protein concentration determination. Analysis was carried out using the ASTRA software (Wyatt Technologies). The dn/dc (change in refractive index as a function of protein concentration, analogous to an extinction coefficient) is approximately constant for proteins and was set to 0.185 [17].

2.4. Equilibrium ultracentrifugation

Ultracentrifugation was performed at 4°C using a Beckman Optima XL-I analytical ultracentrifuge in absorbance mode. Protein samples were in 10 mM Na phosphate pH 8.4, 300 mM NaCl. Three concentrations were used for each sample. For the Sso1:Sec9c complex, the three concentrations were: 2.28 μM, 1.51 μM, and 0.77 μM. For the Sso1:Sec9c:Snc1 complex, the three concentrations were: 3.53 μM, 2.34 μM, and 1.19 μM. A partial specific volume of 0.72 ml/g was used for the binary and ternary complexes. The solvent density used was 1.0075 g/ml. Six sector cells were used to collect data at multiple speeds and at multiple concentrations. Data sets for each protein were subjected to global analysis using the MICROCAL ORIGIN software (Beckman).

2.5. CD spectroscopy

Far UV CD spectra were recorded on an AVIV model 62DS CD spectrometer at 25°C in a 0.1 mm Hellma quartz cuvette. Five scans from 280 nm to 200 nm with averaging time of 1 s and step size of 0.5 nm were averaged. Purified proteins or complexes were dialyzed against 10 mM phosphate buffer pH 8.4 containing 300 mM NaCl. Protein concentrations were determined by internally standardized amino acid analysis following acid hydrolysis (performed by the W.M. Keck Foundation Biotechnology Resource Laboratory at Yale University). For evaluation of changes in the CD spectrum attributable to complex formation, the theoretical non-interacting spectrum was calculated from that of the individual proteins by $\Theta = \Sigma_{n_i} * \Theta_i / \Sigma_{n_i}$ where n_i denotes the number of amino acids in protein i and Θ_i is the observed mean residue ellipticity of protein i. Relative stoichiometries of 1:1 for the binary complex, and of 1:1:1 for the ternary complex were assumed (Fig. 1, equilibrium ultracentrifugation, and [18]). Thermal denaturation was performed in the same cuvette, with measurements taken every 1° between 25 and 95, with 1 min equilibration and 30 s averaging.

2.6. Fluorescence spectroscopy

Emission spectra were obtained at 25°C on a SPEX Fluoromax fluorometer with Snc1 at a concentration of 2.5 μM in 10 mM Na phosphate pH 8.4, 300 mM NaCl. A 100 μl cuvette was used (Hellma). Binary complex was added to indicated concentrations. Samples were equilibrated for several hours at 25°C, and excited at 295 nm in order to exclude any tyrosine fluorescence. Emission spectra were recorded between 305 and 400 nm using a 1 nm step size and 5 s integration time.

2.7. Estimation of binding constants

For the Sso1:Sec9c complex, equilibrium ultracentrifugation showed that the proteins were predominantly associated in the concentration range studied. Since the highest starting concentration of the sample was 2.3 μM (see above), this implies that for the equilibrium Sso1+Sec9c ⇌ Sso1:Sec9c, the dissociation constant is given by $K_D < ([1-x][1-x])/x \cdot 2.3$ μM, where x is close to 1. Making the conservative estimate that complex assembly was around 90% complete (i.e. $x \approx 0.9$) we obtain $K_D < 50$ nM.

For the Sso1:Sec9c:Snc1 complex, the fluorescence intensity increased linearly with binary complex concentration up to saturation. Making similar arguments as above, this time concerning the equilibrium Sso1:Sec9c+Snc1 ⇌ Sso1:Sec9c:Snc1, and using a concentration of 2.5 μM (see above), we obtain $K_D < 50$ nM.

3. Results

3.1. Construction of a synthetic gene coding for Sec9

All attempts to express a GST fusion with the SNAP-25-like domain of Sec9 (residues 401–651, hereafter referred to as Sec9c) failed (P.B., unpublished). The codon usage of Sec9c suggested that a high number of rare codons (notably 26 rare AGG and AGA arginine codons) was responsible for the poor expression in bacteria. We optimized the codon usage by preparing a synthetic gene (see Section 2) which allowed production of Sec9c in sufficient quantities.

3.2. Coiled coil predictions are not well conserved

It has been suggested, based on primary sequence analysis, that SNARE proteins interact with each other via coiled coil domains [6,19–22]. We have examined the predicted propen-

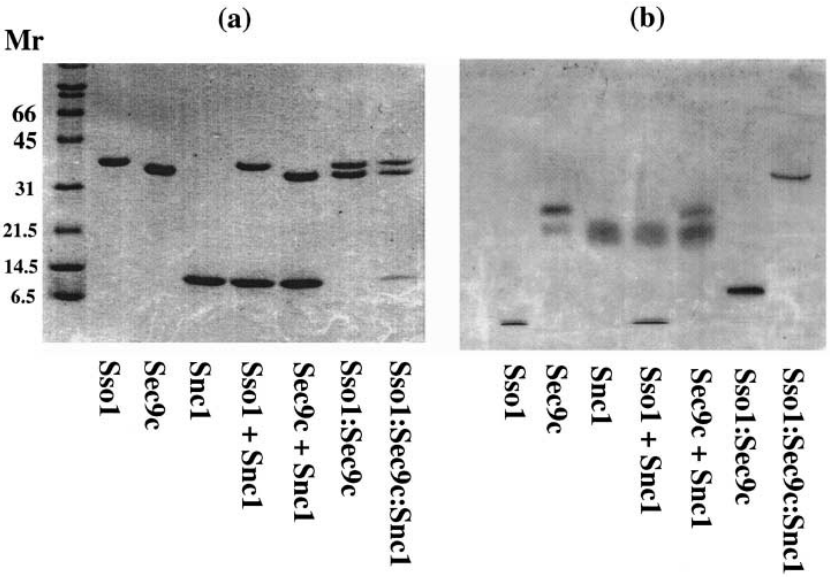

Fig. 1. SDS and native gels. In both (a) and (b), samples loaded in the lanes marked Sso1:Sec9c and Sso1:Sec9c:Snc1 were purified complexes, i.e. stoichiometric mixtures. A '+' indicates that a roughly equimolar amount of the indicated proteins was loaded, but a stable complex was not formed and therefore not purified. (a) 20% SDS gel electrophoresis of individual SNARE proteins, of all pairwise combinations, and of the three-way combination. 1 μl of each sample was loaded on the Phast gel (Pharmacia). Concentrations of the samples were between 0.5 and 1.5 mg/ml. (b) 4–15% native gel electrophoresis on individual SNARE proteins, of all pairwise combinations, and of the three-way combination. Samples (1 μl) were applied directly to a 4–15% gradient Phast gel (Pharmacia).

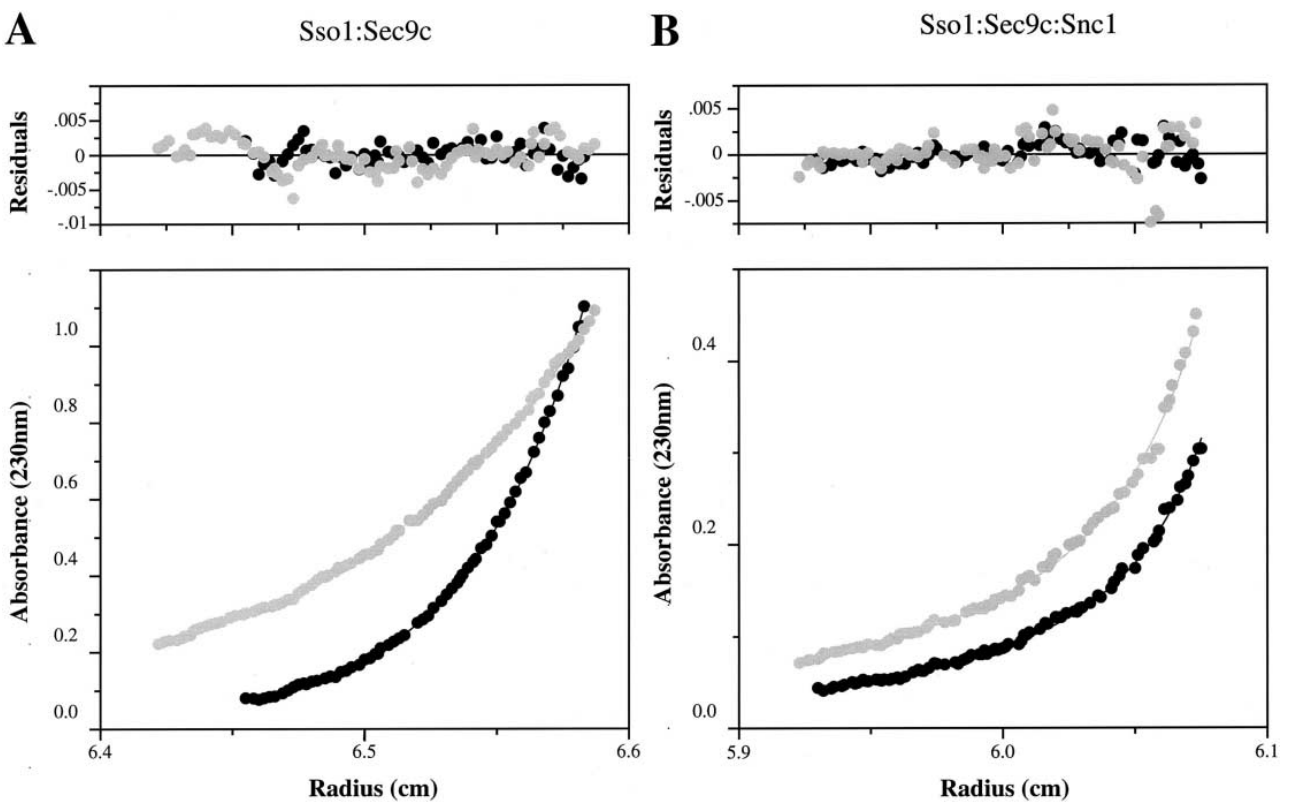

Fig. 2. Determination of the oligomerization state of the Sso1:Sec9c and Sso1:Sec9c:Snc1 complexes. The binary complex behaves as a 1:1 heterodimer, and the ternary complex tends to self-associate. A: Representative sedimentation equilibrium data for the purified Sso1:Sec9c complex at rotor speeds of 13 300 rpm (grey circles) and 20 000 rpm (black circles). Solid lines show the global fit of a single species of M_r 66 kDa to data for all concentrations (see Section 2) at both rotor speeds. B: Representative sedimentation equilibrium data for the purified ternary complex at rotor speeds of 13 000 rpm (grey circles) and 16 000 rpm (black circles). Solid lines show a global fit to a monomer-tetramer equilibrium, where the monomer is assumed to be a 1:1:1 Sso1:Sec9c:Snc1 complex of M_r 70 kDa. The fit was performed using data for all concentrations (see Section 2) at both rotor speeds. This model (goodness of fit 1.46) is nearly indistinguishable from a monomer-pentamer model (goodness of fit 1.48).

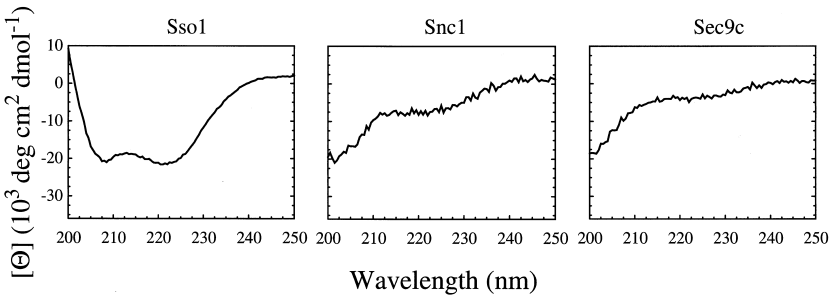

Fig. 3. CD spectra of individual SNARE proteins. CD spectra (mean residue ellipticity [Θ]) were recorded in 10 mM Na phosphate pH 8.4, 300 mM NaCl at 25°C. Sso1 appears to have significant secondary structure content while Sec9c and Snc1 do not. Concentrations are: Sso1, 3.1 μM, Snc1, 5.9 μM, Sec9, 1.4 μM.

sity of the yeast SNARE proteins to form coiled coils using the COILS [23] and the PAIRCOIL [24] programs (not shown). For the yeast proteins, the coiled coil scores are fairly weak. There is also significant variation in the predictions depending on which species or which algorithm is used. It is thus possible that these proteins do not form coiled coils at all, or that they form non-canonical coiled coils that are not well predicted by existing algorithms.

3.3. Changes in mobility in native gel electrophoresis

As a first step towards characterizing the yeast SNARE proteins, we performed native gel electrophoresis (Fig. 1). The only detectable binary interaction occurred between Sso1 and Sec9c, consistent with results obtained using a GST fusion binding assay [18]. All three proteins were quantitatively incorporated into a stable ternary complex. Sso1, the purified binary complex of Sso1 and Sec9c, and the purified ternary complex of Sso1, Sec9c, and Snc1 all migrate as well-defined bands on the native gel. Sec9c and Snc1 run as diffuse bands and, surprisingly, penetrate the gel much less than Sso1. These differences in mobility probably do not result entirely from charge effects since these three proteins do not have greatly different isoelectric points (Sso1: 5.04, Sec9: 5.71, Snc1: 6.80). Instead, they could be due to conformational effects (see below). Unlike the neuronal ternary SNARE complex [6], the yeast ternary complex is not resistant to SDS, even at room temperature (not shown).

Since the electrophoretic separation in a native gel depends simultaneously on charge and size, our assay potentially provides some information about the conformation of the individual proteins and their complexes. For example, the dramatically different mobilities of Sso1 and Sec9c upon native gel electrophoresis (Fig. 1) make it likely that Sso1 adopts a much more compact conformation than Sec9c. Similarly, the mobility of Snc1 would suggest that it might adopt a fairly non-compact, extended conformation. Formation of higher order oligomers as an explanation of the low mobilities of Sec9c and Snc1 can be ruled out because the individual SNAREs are monomeric (see below).

The mobilities of the Sso1:Sec9c complex and of the Sso1:Sec9c:Snc1 complex differ from any of the monomers. The Sso1:Sec9c complex migrates closer to Sso1 than Sec9c, a striking change most likely explained by conformational changes that make the Sso1:Sec9c complex significantly more compact than Sec9c. The Sso1:Sec9c:Snc1 complex migrates slowest of all. Its mobility is substantially different from that of the binary complex. One explanation for the low mobility of the ternary complex is multimerization (see below).

3.4. Individual SNAREs and the Sso1:Sec9c complex are monomeric; the Sso1:Sec9c:Snc1 complex self-associates

Sso1, Sec9c, and Snc1 migrate anomalously on size exclusion columns compared to standards of known molecular weight (not shown). In contrast to size exclusion chromatography, multi-angle laser light scattering [25] can be used to obtain the absolute molecular weight of a macromolecule without making any assumptions about its shape. Using this technique, all three SNAREs were shown to be monomeric (not shown). Equilibrium ultracentrifugation (in contrast to density gradient centrifugation) can also be used to obtain absolute molecular weights, and was used to investigate the association state of the Sso1:Sec9c complex, and of the Sso1:Sec9c:Snc1 complex (Fig. 2A and B respectively). The data for the purified binary complex were well fit by assuming a single, heterodimeric species of about 66 kDa, in good agreement with the theoretical molecular weight of the binary complex of 60 kDa. The data for the purified ternary complex could not be well fit by assuming a single heterotrimeric species of 70 kDa; this assumption clearly underestimated the average molecular weight of the sample. The data from the

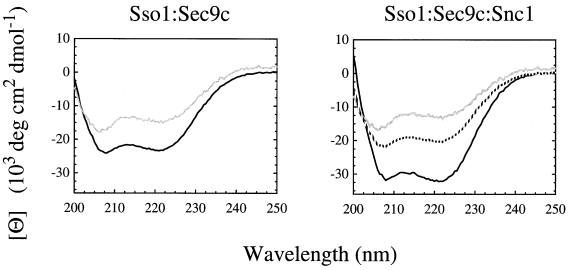

Fig. 4. Changes in the CD spectra resulting from formation of the Sso1:Sec9c complex or of the Sso1:Sec9c:Snc1 complex. CD spectra were recorded under identical conditions as in Fig. 3. Grey lines show the mean residue elipticity predicted for a theoretical, non-interacting mixture (see Section 2) of the individual component proteins. At right, the dashed line shows the mean residue ellipticity predicted for a theoretical, non-interacting mixture (see Section 2) of the binary complex with Snc1. Solid black lines show the observed mean residue ellipticity. For both complexes, the observed mean residue ellipticity exceeds that predicted from theoretical, non-interacting mixtures, suggesting that formation of the Sso1:Sec9c complex and of the Sso1:Sec9c:Snc1 complex induces structure in some of the component proteins. Left panel: Sso1:Sec9c, 3.4 μM, right panel: Sso1:Sec9c:Snc1, 1.35 μM.

two highest centrifugation speeds could be reasonably well fit assuming a single heterotrimeric species of 70 kDa in equilibrium with a tetramer (4:4:4), or pentamer (5:5:5) of heterotrimers. Our data are not sufficient to fit a unique model of the oligomerization state, but clearly indicate that the SNARE complex has a tendency to self-associate. This tendency to self-associate was confirmed by multi-angle laser light scattering (not shown) and is a property specific to the ternary complex since none of the component proteins, or the binary complex, self-associate.

3.5. Circular dichroism spectra indicate structural changes

The individual SNAREs, the Sso1:Sec9c complex, and the Sso1:Sec9c:Snc1 complex are all well-defined entities (Figs. 1 and 2) that can be isolated chromatographically. CD spectroscopy can therefore be used to investigate possible structural changes that may accompany binding events. Far UV CD spectra for Sso1, Sec9c, and Snc1 are shown in Fig. 3. The spectrum for Sso1 shows minima at 222 nm and 208 nm, the characteristic signature of α-helical, or mixed α-helical/β-sheet proteins [26]. The spectra for Sec9c and Snc1 are very similar to each other and are suggestive of largely random coil conformation. The unstructured state of Sec9c and Snc1 was recently confirmed by ongoing NMR studies (Fiebig et al., unpublished).

Fig. 4 (left panel) shows the CD spectrum of the purified complex of Sso1 and Sec9c (t-SNARE complex). It again displays the two minima characteristic of α-helical or mixed α-helical/β-sheet proteins. The observed spectrum is compared to the theoretical non-interacting spectrum obtained from the individual spectra of Sso1 and Sec9c assuming 1:1 stoichiometry (see Section 2). The difference between the theoretical non-interacting and the observed spectra suggests that the formation of the binary complex results in a significant increase in secondary structure, which could arise from induction of structure in Sso1, Sec9c, or both. Fig. 4 (right panel) shows the CD spectrum recorded from the purified ternary complex. It too shows a significant α-helical signal, in large excess of that expected from computing the theoretical non-interacting CD spectrum from spectra of the three individual proteins, or from the observed Sso1:Sec9c complex spectrum and that of Snc1. Again, this increase in mean residue ellipticity could result from increases in any of the individual

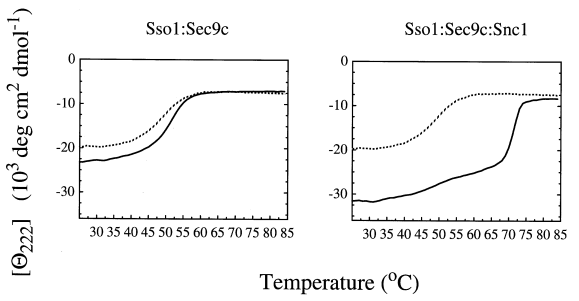

Fig. 5. Thermal stability of Sso1 and of the Sso1:Sec9c and Sso1:Sec9c:Snc1 complexes. Change in mean residue ellipticity at 222 nm (Θ_{222}) was measured as a function of temperature. Buffer conditions were as in Figs. 3 and 4. Measurements were made at 1° temperature increments after 1 min of equilibration, and averaged for 30 s. The dashed line shows the denaturation profile for Sso1 in both panels. Left panel: thermal denaturation profiles for Sso1 and the Sso1:Sec9c complex (solid line), right panel: thermal denaturation profiles for Sso1 and the Sso1:Sec9c:Snc1 complex (solid line).

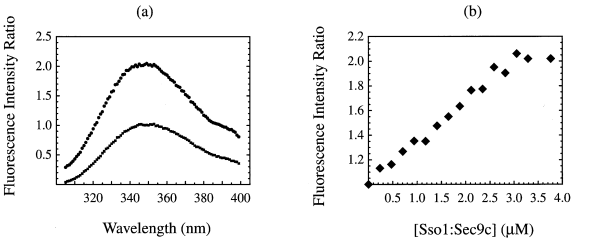

Fig. 6. Changes in tryptophan fluorescence resulting from formation of the Sso1:Sec9c:Snc1 complex. The fluorescence intensity ratio is the measured fluorescence intensity divided by the fluorescence intensity of 2.5 μM Snc1 at 350 nm. The increase in fluoresence intensity is saturable, and up to saturation increases linearly with Sso1:Sec9c complex concentration, suggesting very tight binding. All measurements were performed at 25°C. (a) Emission spectra of Snc1 (2.5 μM) (lower line) and of Snc1 (2.5 μM) combined with purified Sso1:Sec9c complex (3.2 μM) (upper line). (b) Increase in fluorescence intensity ratio as a function of Sso1:Sec9c complex concentration.

protein's secondary structure content although most of the changes are likely to occur in Sec9c and in Snc1. The high mean residue ellipticity observed for the ternary complex suggests a large α-helical content.

As a first step towards characterizing the energetics of SNARE assembly, we have measured thermal denaturation profiles of Sso1, the Sso1:Sec9c complex, and the Sso1:Sec9c:Snc1 complex. Fig. 5 (left panel) shows the thermal denaturation profiles for Sso1 and the binary Sso1:Sec9c complex, and Fig. 5 (right panel) shows the thermal denaturation profiles for Sso1 and the ternary Sso1:Sec9c:Snc1 complex. Sso1 melts with a single transition with a T_m of about 48°C. The Sso1:Sec9c complex also unfolds in a single transition with a T_m of about 50°C. The melting profile of the ternary complex is more complicated, but it shows a cooperative transition at about 71°C.

3.6. Increase in tryptophan fluorescence upon formation of the Sso1:Sec9c:Snc1 complex

There is a single tryptophan in the Sso1:Sec9c:Snc1 complex, at position 86 in Snc1 which is close to (within ten residues) its putative transmembrane domain. Fig. 6 shows the result of titrating Snc1 with increasing amounts of binary complex. Formation of the ternary complex causes a significant increase in fluorescence intensity. The increase in fluorescence is saturable and up to saturation is linear with concentration. This behavior could be explained by tight binding and by structural re-arrangements in the vicinity of the tryptophan residue.

4. Discussion

The importance of the SNARE proteins in vesicular trafficking and fusion is widely accepted based on direct experimental evidence from yeast genetics [11,13,14,16] and from studies of higher eukaryotes [27,28]. The precise function of the SNARE proteins, however, has yet to be determined despite an increasing number of experiments performed in vitro with mammalian SNAREs [6,19–22,29]. In order to gain insight into their function, we have performed an extensive biophysical characterization of the distantly related yeast SNAREs Sso1, Sec9c, and Snc1 and of their complexes. Identification of evolutionarily conserved structural and energetic

properties of SNARE proteins should aid in elucidating a common mechanism for their function in membrane fusion.

All in vitro yeast SNARE binding assays to date have been performed using GST fusion proteins [18]. Here we studied complexes of the yeast SNARE proteins in solution without fusion protein partners. The native gel assay used to examine interactions between the yeast SNARE proteins showed that the only dimeric interaction observed occurs between the two t-SNAREs, Sso1 and Sec9c; comparable results have been obtained from similar studies using neuronal proteins (Fasshauer et al., submitted). We also observe a stable ternary complex that can be purified chromatographically and that gives rise to a single band of very low but well-defined mobility on a native gel (Fig. 1).

We found significantly higher binding affinities than previously reported. Using our data we were able to estimate dissociation constants for the binary and ternary complexes. The purified t-SNARE complex behaved as a well-defined heterodimer of about 66 kDa during equilibrium ultracentrifugation (Fig. 2A) implying that it is predominantly associated and has a 1:1 stoichiometry. This leads to an estimate of the dissociation constant for Sec9c binding to Sso1 at lower than 50 nM (see Section 2). The formation of the ternary complex is accompanied by a large increase in the intrinsic fluorescence of the only tryptophan in the ternary complex, W86 of Snc1 (Fig. 6), and we used this signal to estimate that the dissociation constant for Snc1 binding to the binary Sso1:Sec9c complex is also lower than 50 nM (see Section 2).

The binary complex of Sso1 and Sec9c showed significantly increased mean residue ellipticity compared to a theoretical, non-interacting mixture of the individual proteins (Fig. 4, left panel). Formation of the ternary complex is accompanied by yet another dramatic increase in mean residue ellipticity (Fig. 4, right panel). These results suggest that large conformational changes occur when SNARE proteins bind each other. Our data does not specify which proteins acquire structure, but most of the changes probably occur in Sec9c and in Snc1 because they are the least structured on their own. In terms of thermal stability, the binary Sso1:Sec9c complex is only marginally (if at all) stabilized compared to Sso1, while the ternary complex shows a significantly elevated thermal stability.

The dramatic structural re-arrangements provide several possible explanations for the origin of the tryptophan fluorescence signal. The increase in fluorescence intensity probably results from a change in the environment of the tryptophan, for example protection from collisional quenching by water. When the ternary complex forms, Snc1 could become structured such that it folds onto itself and buries its own tryptophan. Alternatively, the environment of the tryptophan could change due to an oligomerization process. Finally, the proximity of the binary complex could be responsible for the change in environment of the tryptophan. This could have dramatic consequences concerning the geometry of the ternary complex, and might imply that formation of the ternary complex brings the vesicle and plasma membrane in close proximity, perhaps even initiating or directly participating in the fusion event.

The self-association of the 1:1:1 ternary complex into higher order oligomers could have important consequences for the fusion process. Oligomerization could be important in stabilizing the vesicle while docked to the target membranes and/or could aid in the formation of a fusion pore. Interestingly, multimerization of influenza virus fusion protein hemagglutinin trimers has also been observed and has been speculated to play an important role in the fusion event [30].

The finding that Sec9c and Snc1 are unstructured is a striking one, and we believe these unstructured states to be biologically relevant for several reasons. First, the unstructured Snc1 and Sec9c are soluble with no sign of aggregation even at high concentration (K. Fiebig, unpublished), and the Sec9c construct likely represents an independent domain because in the full-length protein it is preceded by a glutamine rich linker region. Second, Sec9c and Snc1 are quantitatively incorporated into a ternary complex when combined with the third SNARE, Sso1. Third, similar unstructured states have been observed with neuronal SNAREs. Finally, the recombinant ternary complex is functional in the sense that it can bind Sec17 (the yeast SNAP) with identical stoichiometry as the neuronal SNARE complex [18]. An unfolded state, even if transient, could couple the energetics of protein folding to that of vesicle docking or perhaps contribute to the fusion event itself. Unfolded to folded transitions have been suggested to play an important role in other macromolecular recognition events, for example in site-specific DNA binding [31]. These transitions were suggested to contribute to the specificity of the recognition. It is intriguing to speculate that the unstructured state of some SNARE proteins, and the induction of structure upon binding, may be conserved biophysical properties that could have a functional role in the docking and fusion process.

Acknowledgements: We thank Isaiah Arkin, Dirk Fasshauer, Lino Gonzales, Sarah Stallings, Richard Yu, Don Engelman, Reinhard Jahn, and Peter Novick for stimulating discussions, Karen Fleming for help with the ultracentrifugation, and William Eliason for help with the multi-angle laser light scattering. L.M.R. is an HHMI predoctoral fellow. This work was in part supported by a grant from the National Institutes of Health (ATB, GM54160-01).

References

[1] Ferro-Novick, S. and Jahn, R. (1994) Nature 370, 191–193.
[2] Südhof, T.C. (1995) Nature 375, 645–653.
[3] Sollner, T., Whiteheart, S.W., Brunner, M., Erdjument-Bromage, H., Geromanos, S., tempst, P. and Rothman, J.E. (1993) Nature 362, 318–324.
[4] Sollner, T., Bennett, M.K., Whiteheart, S.W., Scheller, R.H. and Rothman, J.E. (1993) Cell 75, 409–418.
[5] Hayashi, T., Yamasaki, S., Nauenburg, S., Binz, T. and Neimann, H. (1994) EMBO J. 14, 2317–2325.
[6] Hayashi, T., McMahon, H., Yamasaki, S., Binz, T., Hata, Y., Südhof, T.C. and Niemann, H. (1994) EMBO J. 13, 5051–5061.
[7] Block, M.R., Glick, B.S., Wilcox, C.A., Wieland, F.T. and Rothman, J.E. (1988) Proc. Natl. Acad. Sci. USA 85, 7852–7856.
[8] Hanson, P.I., Otto, H., Barton, N. and Jahn, R. (1995) J. Biol. Chem. 270, 16955–16961.
[9] Rothman, J.E. and Warren, G. (1994) Curr. Biol. 4, 220–233.
[10] Mayer, A., Wickner, W. and Haas, A. (1996) Cell 85, 83–94.
[11] Nichols, B.J., Ungerman, C., Pelham, H.R.B., Wickner, W.T. and Haas, A. (1997) Nature 387, 199–202.
[12] Otto, H., Hanson, P.I. and Jahn, R. (1997) Proc. Natl. Acad. Sci. USA, in press.
[13] Aalto, M.K., Ronne, H. and Keranen, S. (1993) EMBO J. 12, 4095–4104.
[14] Brennwald, P., Kearns, B., Chapion, K., Keranen, S., Bankaitis, V. and Novick, P. (1994) Cell 79, 245–258.
[15] Gerst, J.E., Rodgers, L., Riggs, M. and Wigler, M. (1992) Proc. Natl. Acad. Sci. USA 89, 4338–4342.

[16] Protopopov, V., Govindan, B., Novick, P. and Gerst, J.E. (1993) Cell 74, 855–861.
[17] Wen, J., Arakawa, T. and Philo, J.S. (1996) Anal. Biochem. 240, 155–166.
[18] Rossi, G., Salminen, A., Rice, L.M., Brünger, A.T. and Brennwald, P. (1997) J. Biol. Chem. 272, 16610–16617.
[19] Calakos, N., Bennett, M.K., Peterson, K.E. and Scheller, R.H. (1994) Science 263, 1146–1149.
[20] Pevsner, J., Hsu, S.-C., Braun, J.E.A., Calakos, N., Ting, A.E., Bennett, M.K. and Scheller, R.H. (1994) Neuron 13, 535–561.
[21] Kee, Y., Lin, R.C., Hsu, S.-C. and Scheller, R.H. (1995) Neuron 14, 991–998.
[22] Chapman, E.R., An, S., Barton, N. and Jahn, R. (1994) J. Biol. Chem. 269, 27427–27432.
[23] Lupas, A., van Dyke, M. and Stock, J. (1991) Science 252, 1162–1164.
[24] Berger, B., Wilson, D.B., Wolf, E., Tonchev, T., Milla, M. and Kim, P.S. (1995) Proc. Natl. Acad. Sci. USA 92, 8259–8263.
[25] Wyatt, P. (1993) Anal. Chim. Acta 272, 1–40.
[26] Venyaminov, S.Y. and Yang, J.T. (1996) in: Circular Dichroism and the Conformational Analysis of Biomolecules (Fasman, G.D., Ed.), pp. 69–109, Plenum Press, New York.
[27] Blasi, J., Binz, T., Yamasaki, S., Link, E., Niemann, H. and Jahn, R. (1994) J. Physiol. 88, 235–241.
[28] Broadie, K., Prokop, A., Bellen, H.J., O'Kane, C.J., Schulze, K.L. and Sweeney, S.T. (1995) Neuron 15, 663–673.
[29] Fasshauer, D., Bruns, D., Shen, B., Jahn, R. and Brunger, A.T. (1997) J. Biol. Chem. 272, 4582–4590.
[30] Danieli, T., Pelletier, S.L., Henis, Y.I. and White, J.M. (1996) J. Cell Biol. 133, 559–569.
[31] Spolar, R.S. and Record Jr., M.T. (1994) Science 263, 777–784.